Experimental Animals
Exp. Anim. 73(3), 286–292, 2024

Original

Deletion of *Exoc7*, but not *Exoc3*, in male germ cells causes severe spermatogenesis failure with spermatocyte aggregation in mice

Natsuki MIKAMI[1)], Chi Lieu Kim NGUYEN[1)], Yuki OSAWA[2)], Kanako KATO[3)], Miyuki ISHIDA[3)], Yoko TANIMOTO[3)], Kento MORIMOTO[4,5)], Kazuya MURATA[3)], Woojin KANG[3)], Fumihiro SUGIYAMA[3)], Masatsugu EMA[6)], Satoru TAKAHASI[3)] and Seiya MIZUNO[3)]

[1)]*Program in Human Biology, School of Integrative and Global Majors, University of Tsukuba, 1-1-1 Tennodai, Tsukuba, Ibaraki 305-8575, Japan*
[2)]*Master's Program in Medical Sciences, Graduate School of Comprehensive Human Sciences, University of Tsukuba, 1-1-1 Tennodai, Tsukuba, Ibaraki 305-8575, Japan*
[3)]*Laboratory Animal Resource Center and Trans-Border Medical Research Center, University of Tsukuba, 1-1-1 Tennodai, Tsukuba, Ibaraki 305-8575, Japan*
[4)]*Doctoral Program in Medical Sciences, Graduate School of Comprehensive Human Sciences, University of Tsukuba, 1-1-1 Tennodai, Tsukuba, Ibaraki 305-8575, Japan*
[5)]*Research Fellow of the Japan Society for the Promotion of Science, Kojimachi Business Center Building, 5-3-1 Kojimachi, Chiyoda-ku, Tokyo 102-0083, Japan*
[6)]*Department of Stem Cells and Human Disease Models, Research Center for Animal Life Science, Shiga University of Medical Science, Seta, Tsukinowa-cho, Otsu, Shiga 520-2192, Japan*

Abstract: Vesicular trafficking is essential for the transport of intracellularly produced functional molecules to the plasma membrane and extracellular space. The exocyst complex, composed of eight different proteins, is an important functional machinery for "tethering" in vesicular trafficking. Functional studies have been conducted in laboratory mice to identify the mechanisms by which the deletion of each exocyst factor affect various biological phenomena. Interestingly, each exocyst factor-deficient mutant exhibits a different phenotype. This discrepancy may be due to the function of the exocyst factor beyond its role as a component of the exocyst complex. Male germline-specific conditional knockout (cKO) mice of the *Exoc1* gene, which encodes one of the exocyst factors EXOC1 (SEC3), exhibit severe spermatogenesis defects; however, whether this abnormality also occurs in mutants lacking other exocyst factors remains unknown. In this study, we found that exocyst factor EXOC3 (SEC6) was not required for spermatogenesis, but depletion of EXOC7 (EXO70) led to severe spermatogenesis defects. In addition to being a component of the exocyst complex, EXOC1 has other functions. Notably, male germ cell-specific *Exoc7* cKO and *Exoc1* cKO mice exhibited phenotypic similarities, suggesting the importance of the exocyst complex for spermatogenesis. The results of this study will contribute to further understanding of spermatogenesis from the aspect of vesicular trafficking.
Key words: exocyst complex, intercellular bridges, mouse spermatogenesis, spermatocyte

Introduction

Exocyst complex is a hetero-octamer composed of eight different proteins (EXOC1–8), and the eight genes (*Exoc1–Exoc8*) encoding these proteins are highly conserved in fungi, plants, and animals. The exocyst complex is crucial for the "tethering" of vesicle trafficking [1]. Tethering is a phenomenon in which vesicles from

(Received 7 December 2023 / Accepted 31 January 2024 / Published online in J-STAGE 7 February 2024)
Corresponding author: S. Mizuno. email: konezumi@md.tsukuba.jp
Supplementary Tables: refer to J-STAGE: https://www.jstage.jst.go.jp/browse/expanim

the Golgi apparatus and recycling endosomes are tethered to the plasma membrane during exocytosis. After tethering, the SNARE complex fuses the vesicle membrane with the plasma membrane, and the proteins within the vesicle are either released into the extracellular space or localized to the plasma membrane.

The structure and formation of the exocyst complex in cells and the signaling molecules that bind to the exocyst complex are currently being investigated [2–6]. In addition to molecular mechanistic analyses, functional analyses of the effects of the absence of each exocyst factor on mammalian animal phenotypes are being conducted mainly using genetically modified mouse models. *Exoc1*, *Exoc2*, *Exoc4*, and *Exoc8* knockout (KO) mice exhibit embryonic lethality prior to organogenesis. In particular, *Exoc1* KO and *Exoc2* KO mice exhibit lethal peri-implantation, which is the most adverse phenotype [7–9]. Given that the exocyst complex is strongly involved in the essential intracellular event of vesicular trafficking, it makes sense that mice deficient in each exocyst factor would exhibit the severe phenotypes. However, *Exoc6* KO mice only survive until birth [9]. Interestingly, different phenotypes are observed in different *Exoc* KO mice. The fact that depletion of each factor that is a component of the exocyst complex leads to different phenotypes in mice suggests three possibilities. First, some exocyst factors may have other functions in addition to being a component of the exocyst complex. Second, each exocyst factor may function only as a component of the exocyst complex, with different responsibilities. Third, alternate factors that compensate for the functions of some exocyst factors may exist.

We previously reported that male germ cell-specific *Exoc1* cKO mice exhibit severe spermatogenesis failure [10]. In mice and humans, male germ cells in the spermatogonia (except the A_{single} state), spermatocyte, and spermatid differentiation stages are all connected, and this unique connected cell morphology is called as the syncytium [11]. Moreover, the cytoplasms of different cells are connected via controlled incomplete cytoplasmic division, and constricted junctions are called the intercellular bridges (ICBs) [12]. Deletion of *Exoc1* causes resolution of this ICB constricted structure, resulting in the appearance of multinucleated aggregated spermatocytes and aborted spermatogenesis at this stage [10].

EXOC1 is not only a component of the exocyst complex but also contributes to the initiation of SNARE complex formation [13]. In this study, we generated and analyzed mice depleted of EXOC3 and EXOC7, specifically in male germ cells, to determine whether exocyst complex confusion is responsible for spermatocyte aggregation.

Materials and Methods

Animals

ICR and C57BL/6J mice were purchased from The Jackson Laboratory Japan. *Nanos3*$^{tm2.1(cre)Ysa}$/35YsaRbrc (*Nanos3-Cre*) mice were kindly gifted by Dr. Yumiko Saga [14] and obtained from RIKEN BRC (#RBRC02568). We used the B6-*Exoc7*$^{em1(flox)Utr}$ (*Exoc7-flox*) mice generated in our previous study [15].

B6-*Exoc3*$^{em1(flox)Utr}$ (*Exoc3-flox*) mice generated via zygote embryo genome editing with clustered regularly interspaced palindromic repeat (CRISPR)/CRISPR-associated protein 9 (Cas9) (Fig. 1). Two mouse genomic sequences (5′-GAT TCT AAC ATG CTA AGC CT-3′ and 5′-GCA TGA AGT AGT TAT GTC AG-3′) in introns 3 and 4 of *Exoc3* were selected as single guide RNA targets. Each sequence was inserted into the *pX330-mC* plasmid, which carried both the guide RNA and Cas9 expression units [16]. The flox donor plasmid DNA, *pflox-Exoc3*, carried a genomic region 2,711 bp upstream and 2,125 bp downstream of exon 4 of *Exoc3*. Two loxP sequences were inserted 548 bp upstream and 694 bp downstream of exon 4 in the donor vector. The above DNA vectors were isolated, purified, and microinjected into C57BL/6J zygotes, as previously described [16]. Surviving injected zygotes were transferred into the oviducts of pseudopregnant ICR females, and newborns were obtained.

The mice were maintained in plastic cages under specific pathogen-free conditions at 23.5 ± 2.5°C and 52.5 ± 12.5% relative humidity under a 14/10 h light/dark cycle at the Laboratory Animal Resource Center of the University of Tsukuba. The mice had free access to commercial chow (MF diet; Oriental Yeast Co., Ltd., Tokyo, Japan) and filtered water.

Gene expression and phenotypic analyses were performed using 10-week-old male mice.

Homologous comparison

Amino acid sequence homology of proteins was compared using LALIGN (https://www.ebi.ac.uk/Tools/psa/lalign/) under the following conditions: MATRIX: OPTIMA5, GAP OPEN: −12, GAP EXTEND: 0, and E () THRESHOLD: 10. When splicing variants were present, those encoding the most amino acids were selected for analysis.

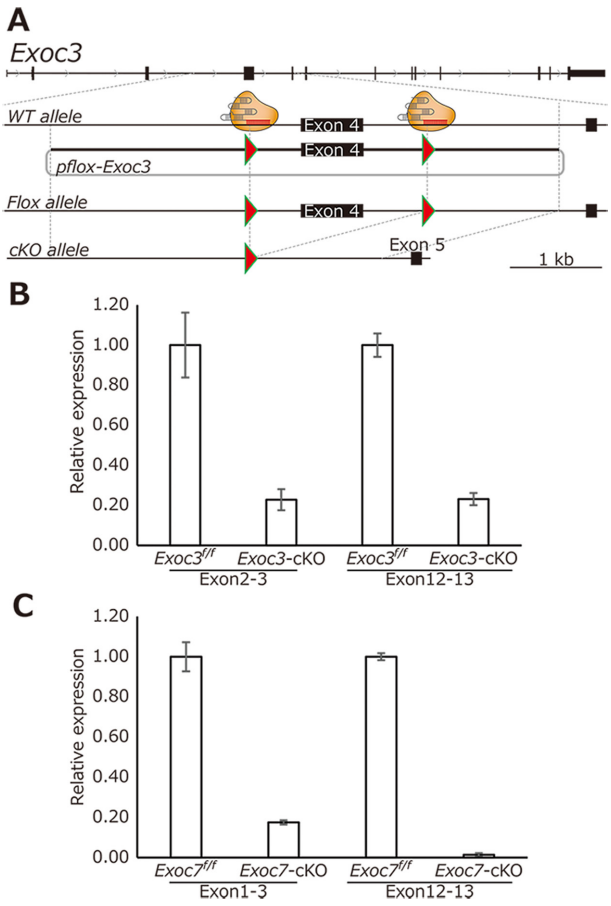

Fig. 1. (A) In the *Exoc3*$^{em1\ (flox)\ Utr}$ (*Exoc3*^{flox}) allele, exon 4 of *Exoc3* gene was floxed. Triangles indicate LoxP. (B) Reverse transcription-quantitative PCR (RT-qPCR) using the RNA extracted from 10-week-old *Exoc3*-conditional knockout (cKO) (*Exoc3*$^{flox/flox}$::*Nanos3*$^{Cre/+}$) and its control (*Exoc3*$^{flox/flox}$) testes (n=3). Exon2–3: RT-qPCR using primers annealing to exons 2 and 3 of *Exoc3* cDNA. Exon12–13: RT-qPCR using primers annealing to exons 12 and 13 of *Exoc3* cDNA. (C) RT-qPCR using the RNA extracted from *Exoc7*-cKO (*Exoc7*$^{flox/flox}$::*Nanos3*$^{Cre/+}$) and its control (*Exoc7*$^{flox/flox}$) testes (n=3). The same format as described above for the description of primers. Exons 8–12 were floxed in the *Exoc7* flox allele.

Quantitative reverse transcription PCR

Total RNA was extracted from the testes using ISOGEN (Nippon Gene, Tokyo, Japan), according to the manufacturer's protocol. Reverse transcription was performed using SuperScript Reverse Transcriptase (Thermo Fisher Scientific, Waltham, MA, USA) and oligo dT primers (Thermo Fisher Scientific). RT-qPCR was performed using the appropriate primers (Supplementary Table 1), SYBR Green PCR Master Mix (Thermo Fisher Scientific), and Thermal Cycler Dice Real Time System III (Takara Bio, Shiga, Japan).

Genotyping PCR

Genomic DNA was extracted from <0.5 mm tails of 3-week-old mice. PCR was performed using the AmpliTaq Gold 360 Master Mix (Thermo Fisher Scientific) with the appropriate primers (Supplementary Table 1). Blastocyst genotyping was performed as previously described [10]. Briefly, each blastocyst was placed in 5 μl of ProK solution (0.02 mg/ml in water), incubated at 55°C for 2 h, and incubated again at 95°C for 7 min. This solution was used as a template for PCR with the AmpliTaq Gold 360 Master Mix and appropriate primers (Supplementary Table 1).

Hematoxylin and eosin (H&E) staining

Testes with the tunica albuginea removed were fixed with the 10%-Formaldehyde Neutral Buffer Solution (Nacalai Tesque, Kyoto, Japan) overnight. Fixed testes were then soaked in 70% ethanol. Embedding in paraffin blocks, preparation of 5-μm sections, and conventional H&E staining were performed as described in our previous report [10]. This test was performed at the Organization Open Facility Initiatives in the University of Tsukuba.

Immunofluorescence and lectin staining

Testis paraffin sections (5 μm) were prepared as described above. After deparaffinization, xylene was removed from the sections using 100% ethanol, and the sections were re-hydrated with 95% ethanol, 70% ethanol, and deionized distilled water. Then, the sections were permeabilized with 0.25% TritonX-100 in phosphate-buffered saline (PBS) and autoclaved (121°C, 10 min) with the Target Retrieval Solution (Agilent Technologies, Santa Clara, CA, USA). The sections were incubated with Blocking One Histo (Nacalai Tesque) for 15 min at room temperature or blocking solution with 0.1% bovine serum albumin, 0.01% Tween20, and 10% goat serum in PBS. Primary antibodies (Supplementary Table 2) diluted with the Can Get Signal Immunoreaction Enhancer Solution A (TOYOBO, Osaka, Japan) or blocking solution were applied, and the sections were incubated for 1 h at room temperature. Alexa Fluor-conjugated secondary antibodies (Supplementary Table 2) were diluted in the same solution as the primary antibodies, and the sections were incubated for 1 h at room temperature. FITC-conjugated lectin from *Arachis hypogaea* (PNA-Lection; Sigma Aldrich Technologies, Darmstadt, Germany) staining was performing with secondary antibody reaction. Nuclear staining with 4',6-diamidino-2-phenylindole (DAPI) was performed using the Prolong Gold Antifade Reagent with DAPI (Thermo Fisher Scientific).

Study approval

All animal experiments were carried out in a humane manner with approval from the Institutional Animal Experiment Committee of the University of Tsukuba in accordance with the Regulations for Animal Experiments of the University of Tsukuba and Fundamental Guidelines for Proper Conduct of Animal Experiments and Related Activities in Academic Research Institutions under the jurisdiction of the Ministry of Education, Culture, Sports, Science, and Technology of Japan (Approval Number: 22-020 and 23-016).

Results

Generation and validation of *Exoc3* and *Exoc7* flox mice

To determine whether the abnormal spermatogenesis exhibited by *Exoc1*-deficient mice [10] is due to the dysfunction of the exocyst complex, we attempted to verify whether other exocyst complex components also played important roles in spermatogenesis in mice. Exocyst complex is a hetero octamer [17]. As the amino acid sequence homology between the exocyst factors (EXOC1–8 proteins) is not high (Supplementary Table 3), each exocyst factor functions as an individual part of the complex rather than functionally compensating for other factors. Although it would be ideal to examine each of the seven factors, except *Exoc1*, extensive effort is required for such analysis. Therefore, we selected *Exoc3* and *Exoc7* for this study. *Exoc3* was selected because it is the most strongly expressed component of the exocyst complex in male germ cells at each stage in mice [18]. *Exoc7* was also selected because, similar to *Exoc1*, it plays a critical role in tethering events by binding to the plasma membrane [3].

Here, C57BL/6J-*Exoc7*$^{em1(flox)Utr}$ (*Exoc7* flox) mice generated in our previous study [15] were used. The 8th to 11th exons were floxed in the *Exoc7* flox mice. We generated C57BL/6J-*Exoc3*$^{em1(flox)Utr}$ (*Exoc3* flox) mice via zygote genome editing. No splice variants have been reported for the mouse *Exoc3* gene, and only the isoform listed in the National Center of Biotechnology Information Reference Sequence Database (RefSeq; https://www.ncbi.nlm.nih.gov/refseq/), NM_ 177333.4, was targeted. This *Exoc3* isoform consists of 13 exons. When the 4th exon is deleted and splicing occurs between the 3rd and 5th exons, a premature termination codon emerges on the 5th exon and nonsense-mediated mRNA decay occurs. Therefore, we generated genome-edited mice by floxing the 4th exon, which is considered the "critical exon" [19] (Fig. 1A).

These *Exoc3* and *Exoc7* flox mice were crossed with *Nanos3-Cre* mice [14], which express Cre in the spermatogonial stem cells, to generate male germline-specific *Exoc3* conditional knockout (cKO) and *Exoc7* cKO mice. To confirm the reduced expression of the target genes, RT-qPCR was performed using primers for exons upstream and downstream of the floxed exon(s). Expression analyses of mRNA extracted from the whole testes revealed a decrease in target gene expression of more than 75% in each case (Figs. 1B and C).

Exoc3 is dispensable for spermatogenesis in mice

We examined whether *Exoc3* cKO (*Exoc3*$^{flox/flox}$::*Nanos3*$^{Cre/+}$) mice also exhibit the abnormal spermatogenesis observed in *Exoc1* cKO (*Exoc1*$^{flox/flox}$::*Nanos3*$^{Cre/+}$) mice. We validated the H&E-stained testis sections of 10-week-old *Exoc3* cKO mice and observed no obvious abnormalities compared with control mice (*Exoc3*$^{+/flox}$::*Nanos3*$^{Cre/+}$; Fig. 2A). The abnormal structure observed in *Exoc1* cKO mice, in which spermatocytes aggregate due to the failure of ICB formation [10], was also not observed in *Exoc3* cKO mice (Fig. 2A). Analysis of H&E-stained sections revealed that the percentage of seminiferous tubules with no spermatids in the lumen was 16.8% (n=3, 9/67, 8/58, and 17/77) in *Exoc3* cKO mice, similar to the percentage of 12.6% (n=3, 9/105, 11/70, and 17/118) in control mice (Fig. 2B). In *Exoc3* cKO mice, the conditional KO efficiency may not be 100% (Fig. 1B). We detected the acrosome with PNA staining and observed no significant abnormalities in *Exoc3* cKO mice (Fig. 1C). To investigate the possibility that only *Exoc3* non-cKO germ cells exhibit normal spermatogenesis, sperms from *Exoc3* cKO male mice were *in vitro* fertilized with oocytes from wild-type female mice, and the genotypes of the blastocyst embryos were confirmed. The cKO allele was identified in the analyzed blastocysts (Fig. 2D). The flox alleles detected in some blastocyst embryos could originate from sperm in which Cre-loxP recombination did not occurred, which was consistent with the result that *Exoc3* conditional KO efficiency was not 100% (Fig. 1B). These results indicate that *Exoc3* is not always required for spermatogenesis.

Exoc7 is indispensable for spermatogenesis in mice

We analyzed the function of *Exoc7* in spermatogenesis using the method as for *Exoc3* described above. We verified the H&E-stained testis sections of 10-week-old *Exoc7* cKO (*Exoc7*$^{flox/flox}$:*Nanos3*$^{Cre/+}$) mice, and almost all seminiferous tubules showed an anomaly in the absence of germ cells on the lumenal side (Fig. 3A).

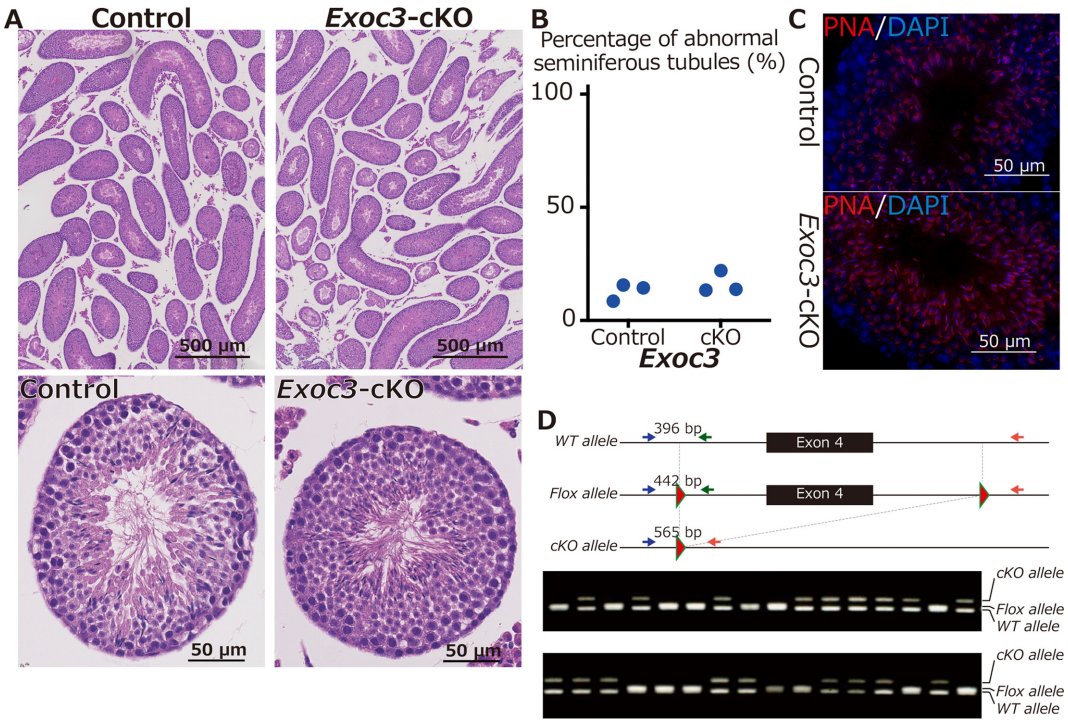

Fig. 2. (A) Panoramic image of hematoxylin and eosin (H&E)-stained testis (upper) and representative seminiferous tubule (bottom) sections in 10-week-old *Exoc3* conditional knockout (cKO) and control mice. (B) Percentage of seminiferous tubules without sperms or spermatids in the testis lumen of 10-week-old *Exoc3* cKO and control mice (each n=3). (C) PNA lectin staining to detect the sperm acrosome. Nuclei were stained with 4',6-diamidino-2-phenylindole (DAPI). Scale bar=50 μm. (D) Genotypic analysis of blastocysts obtained via the *in vitro* fertilization of *Exoc3* cKO sperms and wild-type oocytes. Upper part shows the annealing site of the primer used to detect each allele. Bottom part shows that the flox, wild-type, and cKO alleles were detected as PCR bands of 442, 396, and 565 bp, respectively, by these primers.

Analysis of H&E-stained sections revealed that the percentage of seminiferous tubules with no spermatids in the lumen was very high: 96.9% (n=3, 30/30, 40/42, and 23/24) in *Exoc7* cKO mice and 9.5% (n=3, 8/78, 14/124, and 10/134) in control mice (*Exoc7*$^{+/flox}$::*Nanos3*$^{Cre/+}$; Fig. 3B). Spermatocyte aggregation, which is believed to be the direct cause of spermatogenesis failure in *Exoc1* cKO mice, was also observed in *Exoc7* cKO mice (Figs. 3C and D). Although not considered a cause of spermatogenesis failure, adult *Exoc1* cKO mice show an imbalance in the differentiation of spermatogonia populations: the number of Gfra1-positive spermatogonial cells, which are considered the most undifferentiated, is increased and the number of Rarγ-positive spermatogonial cells, the next stage of differentiation, is decreased [10]. We confirmed whether alterations in the abundance of these cell populations were observed in *Exoc7* cKO mice. The number of Gfra1-positive cells was significantly higher in *Exoc7* cKO mice than in control mice (Figs. 3E and F). But unlike *Exoc1* cKO, the number of Rarγ-positive spermatogonial cells, the next stage of differentiation, also tended to increase, although not significantly (Figs. 3E and F).

These results illustrate that, of the two abnormal phenotypes exhibited by the *Exoc1* cKO mice, spermatocyte aggregation and spermatogonial differentiation imbalance, the former is also observed in *Exoc7* cKO mice.

Discussion

In the present study, we first established *Exoc3* flox mice. Using these *Exoc3* flox mice with our previously established *Exoc7* flox mice, we analyzed the effects of male germ cell-specific deletions in *Exox3* or *Exoc7* on spermatogenesis. *Exoc3* cKO mice did not show any noticeable abnormalities, whereas *Exoc7* cKO mice showed severe spermatogenic defects with spermatocyte aggregation, similar to those observed in *Exoc1* cKO mice. The novel finding of this study is that *Exoc3* deletion does not significantly affect spermatogenesis, whereas *Exoc7* deletion leads to spermatogenesis failure.

In each cKO mouse, *Exoc3* and *Exoc7* showed different degrees of decreased expression (Figs. 1B and C). Although the distance between the two LoxPs affects the recombination efficiency [20], the floxed regions of *Exoc3* and *Exoc7* were 1,954 and 1,547 bp long, respec-

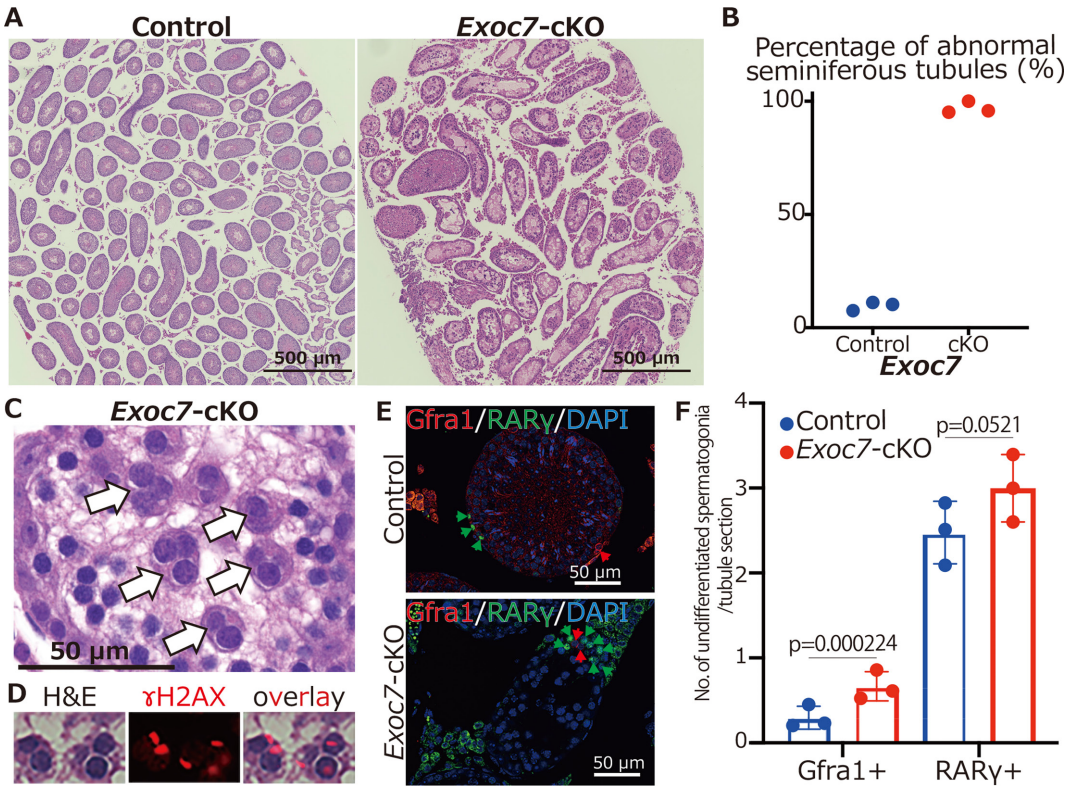

Fig. 3. (A) Panoramic image of hematoxylin and eosin (H&E)-stained testis sections in 10-week-old *Exoc7* conditional knockout (cKO) and control mice. (B) Percentage of seminiferous tubules without sperms or spermatids in the testis lumen of 10-week-old *Exoc7* cKO and control mice (each n=3). (C) Representative image of the sections of the seminiferous tubules of 10-week-old *Exoc7* cKO mice. Aggregated spermatocytes are indicated by the arrows; no sperms were observed. Scale bar=50 μm. (D) Representative image of the aggregated spermatocytes from *Exoc7* cKO mice. Signals of γH2AX, a spermatocyte marker, were observed in the nucleus of the aggregated cells. (E) Representative immunostaining images of Gfra1 (red; red arrows) and Rarγ (green; green arrows), markers of each spermatogonia differentiation stage. Nuclei were stained with 4',6-diamidino-2-phenylindole (DAPI). Scale bar=50 μm. (F) Quantification of Gfra1- or Rarγ-positive cells in each seminiferous tubule in which at least one of the Gfra1-positive or Rarγ-positive cells was present. Both Gfra1- and Rarγ-positive cells were more abundant in the 10-week-old *Exoc7* cKO mice than in the control mice; Student's *t*-test.

tively, with little difference. Both *Exoc3* and *Exoc7* are expressed in Sertoli cells, a non-germ cell lineage [18]. Because expression analysis was performed on bulk testis samples in this study, it is possible that the overall gene expression level was higher in the Sertoli cells of *Exoc3* cKO testes, where spermatogenesis was not impaired, than in those of *Exoc7* cKO testes, where spermatogenesis was impaired. We also cannot exclude the possibility that *Exoc7* mRNA may be more sensitive to nonsense-mediated mRNA decay, although the genomic Cre-loxP recombination efficiencies were similar.

Under similar experimental conditions (same Cre driver mice, genetic background, and age), *Exoc7* cKO mice showed severe spermatogenesis defects with spermatocyte aggregation, similar to *Exoc1* cKO mice. The results of gene function analysis revealed that spermatocyte aggregation was caused by dysfunction of the exocyst complex. Our findings here are consistent with earlier reports that dysfunction of the exocyst complex leads to multinucleation in cultured human cells by impairing the transport of the subunits of the ESCRT III complex [4]. However, this abnormal phenotype was not observed in *Exoc3* cKO mice under similar experimental conditions. This may be because EXOC3 is not as important for the formation and function of the exocyst complex, at least in spermatocytes, as EXOC1 and EXOC7, which bind directly to the plasma membrane. Another possible cause could be the presence of genes that compensate for *Exoc3* function. There are at least four *Exoc3-like* genes: *Exoc3l*, *Exoc3l2*, *Exoc3l4*, and *Tnfaip2*. Although the amino acid sequence homology between EXOC3 and these EXOC3L proteins was not very high (Supplementary Table 4), their functional compensatory potential warrants further investigation.

The mode of abnormal spermatogonia differentiation balance, although not considered a cause of spermato-

genesis defects, differed between the *Exoc1* and *Exoc7* cKO mice. In *Exoc1* cKO mice, the number of Gfra1-positive cells was increased and that of Rarγ-positive cells was decreased [10], whereas both were increased in the *Exoc7* cKO mice. *Exoc7* cKO spermatogonia may be stuck in a Rarγ-positive differentiation state, as they may resist differentiation from Rarγ-positive to Kit-positive spermatogonia cells. Retinoic acid binding to the Rarγ receptor is important in this differentiation process [21], but perhaps there are other important signals, and *Exoc7* may be important in the intracellular trafficking of factors that constitute these unknown signal pathways. This interesting possibility could not be verified as only a simple gene function analysis was performed in this study. In future studies, it is important to determine the molecular mechanisms via the transcriptome analysis of male germ cells at each stage and interactome analysis to identify the factors binding to each exocyst factor.

Acknowledgments

This work was supported by JSPS KAKENHI Scientific Research (B) (19H03142 to S.M.) and JSPS KAKENHI Grant-in-Aid for Scientific Research on Innovative Areas (21H00224 to S.M.) from the Ministry of Education, Culture, Sports, Science, and Technology (MEXT).

References

1. Pfeffer SR. Transport-vesicle targeting: tethers before SNAREs. Nat Cell Biol. 1999; 1: E17–E22. [Medline] [CrossRef]
2. Mei K, Li Y, Wang S, Shao G, Wang J, Ding Y, et al. Cryo-EM structure of the exocyst complex. Nat Struct Mol Biol. 2018; 25: 139–146. [Medline] [CrossRef]
3. Ahmed SM, Nishida-Fukuda H, Li Y, McDonald WH, Gradinaru CC, Macara IG. Exocyst dynamics during vesicle tethering and fusion. Nat Commun. 2018; 9: 5140. [Medline] [CrossRef]
4. Kumar H, Pushpa K, Kumari A, Verma K, Pergu R, Mylavarapu SVS. The exocyst complex and Rab5 are required for abscission by localizing ESCRT III subunits to the cytokinetic bridge. J Cell Sci. 2019; 132: jcs226001. [Medline]
5. Liu DA, Tao K, Wu B, Yu Z, Szczepaniak M, Rames M, et al. A phosphoinositide switch mediates exocyst recruitment to multivesicular endosomes for exosome secretion. Nat Commun. 2023; 14: 6883. [Medline] [CrossRef]
6. Parrini MC, Sadou-Dubourgnoux A, Aoki K, Kunida K, Biondini M, Hatzoglou A, et al. SH3BP1, an exocyst-associated RhoGAP, inactivates Rac1 at the front to drive cell motility. Mol Cell. 2011; 42: 650–661. [Medline] [CrossRef]
7. Mizuno S, Takami K, Daitoku Y, Tanimoto Y, Dinh TT, Mizuno-Iijima S, et al. Peri-implantation lethality in mice carrying megabase-scale deletion on 5qc3.3 is caused by Exoc1 null mutation. Sci Rep. 2015; 5: 13632. [Medline] [CrossRef]
8. Friedrich GA, Hildebrand JD, Soriano P. The secretory protein Sec8 is required for paraxial mesoderm formation in the mouse. Dev Biol. 1997; 192: 364–374. [Medline] [CrossRef]
9. Birling MC, Yoshiki A, Adams DJ, Ayabe S, Beaudet AL, Bottomley J, et al. International Mouse Phenotyping Consortium (IMPC). A resource of targeted mutant mouse lines for 5,061 genes. Nat Genet. 2021; 53: 416–419. [Medline] [CrossRef]
10. Osawa Y, Murata K, Usui M, Kuba Y, Le HT, Mikami N, et al. EXOC1 plays an integral role in spermatogonia pseudopod elongation and spermatocyte stable syncytium formation in mice. eLife. 2021; 10: e59759. [Medline] [CrossRef]
11. Dym M, Fawcett DW. Further observations on the numbers of spermatogonia, spermatocytes, and spermatids connected by intercellular bridges in the mammalian testis. Biol Reprod. 1971; 4: 195–215. [Medline] [CrossRef]
12. Greenbaum MP, Yan W, Wu MH, Lin YN, Agno JE, Sharma M, et al. TEX14 is essential for intercellular bridges and fertility in male mice. Proc Natl Acad Sci USA. 2006; 103: 4982–4987. [Medline] [CrossRef]
13. Yue P, Zhang Y, Mei K, Wang S, Lesigang J, Zhu Y, et al. Sec3 promotes the initial binary t-SNARE complex assembly and membrane fusion. Nat Commun. 2017; 8: 14236. [Medline] [CrossRef]
14. Suzuki H, Tsuda M, Kiso M, Saga Y. Nanos3 maintains the germ cell lineage in the mouse by suppressing both Bax-dependent and -independent apoptotic pathways. Dev Biol. 2008; 318: 133–142. [Medline] [CrossRef]
15. Kuno A, Ikeda Y, Ayabe S, Kato K, Sakamoto K, Suzuki SR, et al. DAJIN enables multiplex genotyping to simultaneously validate intended and unintended target genome editing outcomes. PLoS Biol. 2022; 20: e3001507. [Medline] [CrossRef]
16. Mizuno-Iijima S, Ayabe S, Kato K, Matoba S, Ikeda Y, Dinh TTH, et al. Efficient production of large deletion and gene fragment knock-in mice mediated by genome editing with Cas9-mouse Cdt1 in mouse zygotes. Methods. 2021; 191: 23–31. [Medline] [CrossRef]
17. Koumandou VL, Dacks JB, Coulson RM, Field MC. Control systems for membrane fusion in the ancestral eukaryote; evolution of tethering complexes and SM proteins. BMC Evol Biol. 2007; 7: 29. [Medline] [CrossRef]
18. Green CD, Ma Q, Manske GL, Shami AN, Zheng X, Marini S, et al. A comprehensive roadmap of murine spermatogenesis defined by single-cell RNA-seq. Dev Cell. 2018; 46: 651–667. e10. [Medline] [CrossRef]
19. Skarnes WC, Rosen B, West AP, Koutsourakis M, Bushell W, Iyer V, et al. A conditional knockout resource for the genome-wide study of mouse gene function. Nature. 2011; 474: 337–342. [Medline] [CrossRef]
20. Wang SZ, Liu BH, Tao HW, Xia K, Zhang LI. A genetic strategy for stochastic gene activation with regulated sparseness (STARS). PLoS One. 2009; 4: e4200. [Medline] [CrossRef]
21. Yoshida S. Open niche regulation of mouse spermatogenic stem cells. Dev Growth Differ. 2018; 60: 542–552. [Medline] [CrossRef]